

# Does Gold-Silver Core-Shell Nanostructure with Alginate Coating Induce Apoptosis in Human Lymphoblastic Tumoral (Jurkat) Cell Line?

Jamileh Sadat Mirsanei<sup>#1</sup>, Mahsa Nazari<sup>#1</sup>, Ronak Shabani<sup>2</sup>, Azam Govahi<sup>3</sup>,  
Sahar Eghbali<sup>1</sup>, Marziyeh Ajdary<sup>3</sup>, Rana Mehdizadeh<sup>4</sup>,  
Atieh Sadat Mousavi<sup>1</sup>, Mehdi Mehdizadeh<sup>\*2</sup>

## Abstract

**Background:** T-cell acute lymphoblastic leukemia (T-ALL) is known as an aggressive malignant disease resulting from the neoplastic alteration of T precursor cells. Although treatment with stringent chemotherapy regimens has achieved an 80% cure rate in children, it has been associated with lower success rates in adult treatment. Silver nanoparticles (Ag-NPs) have a toxic effect on human breast cancer cells, human glioblastoma U251 cells, and chronic myeloid leukemia cells in vitro. This study aimed to investigate the effect of Ag nanostructures (Ag-NSs) on Jurkat cells' viability and apoptosis.

**Methods:** The Jurkat cell line was acquired. Following the synthesis Ag-NSs and their characterization, they were incubated with Jurkat cells at different doses for 24, 48, and 72 hours to determine the optimal time and dose. Two groups were examined: a control group with Jurkat cells without nanostructure maintained in the same medium as the cells in the treatment group without changing the medium, and a treatment group with cells treated with the Ag nanostructure solution at a dose of 75 µg/ml for 48 hours according to the MTT results. After 48 hours, the cells from the two groups were used for the q RT-PCR of the apoptotic genes (*BAX*, *BCL-2*, and *CASPASE-3*).

**Results:** According to our results, the rod-shaped silver nanostructures had a size of about 50 nm, increased apoptotic markers, including *BAX* and *CASPASE-3*, and induced cell death.

**Conclusions:** Ag-NSs have anticancer properties and can induce apoptosis of cells; therefore, they may be a potential candidate for the treatment of T-cell acute lymphoblastic leukemia.

**Keywords:** Apoptosis, Cell viability, Nanostructures, T-cell acute lymphoblastic leukemia.

## Introduction

Acute Lymphoblastic Leukemia (ALL) is the most common hematologic malignant disorder (1), which is divided into two subtypes: B-ALL originating from B-cell progenitors and T-ALL arising from T-cell progenitors (2). T-cell acute lymphoblastic leukemia (T-ALL) is an aggressive, malignant lymphoid neoplasm of the T-cell lineage composed of bone

marrow, blood or thymus, and lymph nodes, and it is twice as common in men as in women (3). According to the intrathymic differentiation steps, T-ALL is divided into four subcategories: pro-T-ALL, pre-T-ALL, cortical-T-ALL, and medullary-T-ALL (4). Patients with T-ALL have a poor prognosis arising from an increased risk of the central

1: Department of Anatomy, School of Medicine, Iran University of Medical Sciences, Tehran, Iran.

2: Reproductive Sciences and Technology Research Center, Department of Anatomy, Iran University of Medical Sciences, Tehran, Iran.

3: Endometriosis Research Center, Iran University of Medical Sciences (IUMS), Tehran, Iran.

4: School of Dentistry, Central Tehran Branch, Islamic Azad University, Tehran, Iran.

# The first and the second authors contributed equally to this work.

\*Corresponding author: Mehdi Mehdizadeh; Tel: +98 +98 21 86704543; E-mail: Mehdizadeh.m@iums.ac.ir.

Received: 14 Jan, 2023; Accepted: 24 Sep, 2023

nervous system's engrossment (5). Routine treatment options for T- ALL, such as chemotherapy, have not cured the disease despite high cure rates and long-term durability. Chemoresistance or relapse is the major cause of T- ALL recurrence and death (6). In human cancers, apoptosis evasion, allowing cancer cells to proliferate uncontrollably and develop resistance to chemotherapy (7).

Apoptosis is considered an important mechanism of programmed cell death and plays a role in cell damage, morphogenesis, and normal tissue development (8). Apoptosis can occur in two ways, either by the extrinsic pathway via cell death receptors such as TNF $\alpha$  (tumor necrosis factor- $\alpha$ ), TRIR, and FasL in the cell by stimulating their receptors (TNFR, DR5, and Fas) on another cell or by the intrinsic pathway via the mitochondrial signaling cascade (9, 10).

The BCL-2 protein family members play a critical role in regulating the intrinsic or mitochondrial pathways of apoptosis by interactions determining the integrity of the mitochondrial outer membrane (11).

In the field of nanomedicine, several studies have addressed metal-based nanoparticles (NPs) (12). Among different nanoparticles, silver NPs (Ag-NPs) are of medical interest due to their unique physical, chemical, anticancer, and antimicrobial properties (13). Numerous studies have reported varying degrees of *in vitro* cytotoxicity induced by silver NPs. One of the main toxic effects of silver NPs is triggering programmed cell death, cell apoptosis (14, 15). Some recent reports have confirmed the cytotoxic effect of silver NPs on human breast cancer cells MCF7 (16), human glioblastoma cells U251 (17), and chronic myeloid leukemia cells *in vitro* (18). Lee et al. (19) concluded that Ag-NPs disrupted cellular proliferation and mitochondrial function and induced the apoptosis of NIH3T3 cells (19). In this regard, Ag-NPs are hoped to provide a new strategy to overcome treatments associated with T- ALL.

To our knowledge, there is no report on the anticancer effect of silver NPs on T-ALL. The

Gold-Silver core-shell nanorods were made and examined in this study to investigate the effects on T cell viability on acute lymphoblastic leukemia and cell apoptosis.

## Materials and Methods

### Materials

Ascorbic acid (AA,  $\geq 99.7\%$ ) and Tetrachloroauric acid trihydrate (HAuCl<sub>4</sub>.3H<sub>2</sub>O, 99.9% trace metal basis) were obtained from Sigma-Aldrich (USA). Sodium borohydride (NaBH<sub>4</sub>, 99.99%), silver nitrate (AgNO<sub>3</sub>,  $\geq 99.8\%$ ), sodium hydroxide (NaOH, 97%), cetyltrimethylammonium bromide (CTAB, 99.9%), and sulphuric acid (H<sub>2</sub>SO<sub>4</sub>) were purchased from Merck (Germany).

### Synthesis and Characteristic of Silver Nanostructure

The Gold-Silver core-shell nanostructure was fabricated and then characterized based on our previous report (20).

### Ethical consideration

All experiments were approved by the Research and Ethics Committee of the Iran University of Medical Sciences, Tehran, Iran (IR.IUMS.FMD.REC.1398.033).

### Cell line culture

The Jurkat cell line (human T-ALL) was obtained from the Iranian Biological Resource Center, Tehran, Iran (IBRC). The cells were maintained in the RPMI-1640 medium (Gibco, Invitrogen) which contain fetal bovine serum (10%) (FBS; HyClone; GE Healthcare Life Sciences) and penicillin (1%) (100 U/ml) / streptomycin (100  $\mu$ g/ml) (Gibco, Invitrogen). Cells were then placed in a 5% CO<sub>2</sub> incubator at 37 °C and humidified atmosphere.

### Dosimetry

Since treatment with Ag nanostructure was performed on Jurkat cells, it was necessary to obtain an optimal dose to induce appropriate apoptosis in these cells. Jurkat cells were treated with Ag nanostructure solutions at

different doses and periods. Different concentrations of Ag nanostructure (0, 25, 50, and 75  $\mu\text{g/ml}$ ) were also added to the cultures and incubated for 24, 48, and 72 hours.

### **Cytotoxicity assay**

To determine the effects of nanostructure dose on Jurkat cell line viability and effective time we used the tetrazolium salt 3-(4,5-dimethylthiazol-2-yl)-2,5-diphenyltetrazolium bromide (MTT) (Sigma, Saint Louis, USA) assay. Following the treatment time point, cell viability and half-maximal inhibitory concentration (IC<sub>50</sub>) index were determined using the MTT assay.

Jurkat cells were seeded in 96-well microplates at  $2 \times 10^4$  cells per 200  $\mu\text{l}$  RPMI culture medium and treated with Ag nanostructure solutions at different doses at different intervals. Different concentrations of Ag nanostructure (25, 50, and 75  $\mu\text{g/ml}$ ) were added to the cultures and incubated for 24, 48, and 72 hours. Then the cells (treated/untreated control cells) were centrifuged at 250 RCF for 10 minutes to separate cells and supernatants. The cells were incubated with 150  $\mu\text{l}$  fresh medium and 50  $\mu\text{l}$  MTT solutions (Sigma-Aldrich, USA) (5 mg/mL) for 4 hours at 37 °C and 5% CO<sub>2</sub>, among which the metabolically active cells reduced MTT to blue formazan crystals. Following the incubation period, the medium containing MTT was discarded, and 100  $\mu\text{l}$  DMSO (Sigma-Aldrich) was added to each well and shaken for 15 minutes to dissolve these crystals. The Optical Density (OD) of each sample was measured with a spectrophotometric plate reader at 570 nm (Biotek-refelx800, USA). All experiments were performed in triplicate, the cell score was evaluated using the equation in the Appendix and compared with the control group, and cell viability was expressed as a percentage.

### **Nanostructure treatment**

There were two groups in this experiment: The nanostructure group (group 1) with cells were treated with an Ag nanostructure

solution at a dose of 75  $\mu\text{g/ml}$  for 48 hours according to the MTT results, and the control group (group 2) having Jurkat cells without nanostructure, in the same medium as the cells in the treatment group without changing the medium. After 48 hours, the cells in both groups were used for q RT-PCR.

### **Quantitative RT-PCR Analysis**

The expression level of apoptotic genes including *BAX*, *BCL-2*, and *CASPASE-3* in the Jurkat cell line was assessed using the real-time PCR analysis.

Three gene-specific primer sets and the housekeeping gene *GAPDH* primer were used as reference genes (Table 1). To separate cells and supernatant, control and treated cells were centrifuged at 250 RCF for 5 minutes. Total RNA was then extracted with Trizol (Milipore Sigma, Sigma-Aldrich, USA) and quantified using a Nano-Drop spectrophotometer (Thermo Fisher Scientific Inc., Wilmington, USA). Complementary DNA (cDNA) was synthesized according to the kit protocol (Fermentas Kit, Thermo Fisher Scientific, USA). The standard agarose gel electrophoresis method confirmed the cDNA synthesis. The real-time PCR experiment, performed in triplicate for each sample, was conducted using SYBR Green/ROX dye solution at a volume ratio of 25:1 (Applied Biosystems, OR, USA). Relative expression was generally determined as a fold change from the *GAPDH* level and quantified using the  $2^{-\Delta\Delta C_t}$  method (21).

### **Statistical analysis**

All data were expressed as mean  $\pm$  standard deviation (SD) in at least three specimens. The significance level was set to be  $P \leq 0.05$ . The normal distribution of the data was analyzed using the Kolmogorov-Smirnov test. Then the one-way Analysis of Variance (ANOVA) test was used to determine the significance of the data. All assays were analyzed using GraphPad Prism software version 8 (GraphPad Software, San Diego, CA, USA).

**Table 1.** Primer sequences used in Real-time PCR.

Gene		Sequence (5'to 3')	Length (bp)	T <sub>m</sub> (°C)	PCR product size (bp)
<i>GAPDH</i>	Forward	CTTTGGTATCGTGGAAGGAC	20	55.86	126
	Reverse	GCAGGGATGATGTTCTGG	18	55.07	
<i>BAX</i>	Forward	TTGCTTCAGGGTTTCATCCAGG	23	60.82	174
	Reverse	CACGGCGGCAATCATCCTCT	20	62.93	
<i>BCL-2</i>	Forward	GATAACGGAGGCTGGGATGC	20	60.60	162
	Reverse	GGCATGTTGACTTCACTTGTGG	22	60.29	
<i>CASPASE-3</i>	Forward	CACAGCACCTGGTTATTATTCTTGG	25	60.16	150
	Reverse	TCAAATTCTGTTGCCACCTTTCG	23	60.24	

## Results

The spherical and floating Jurkat cells with regular nuclei grew and reached a reasonable density (Fig. 1).

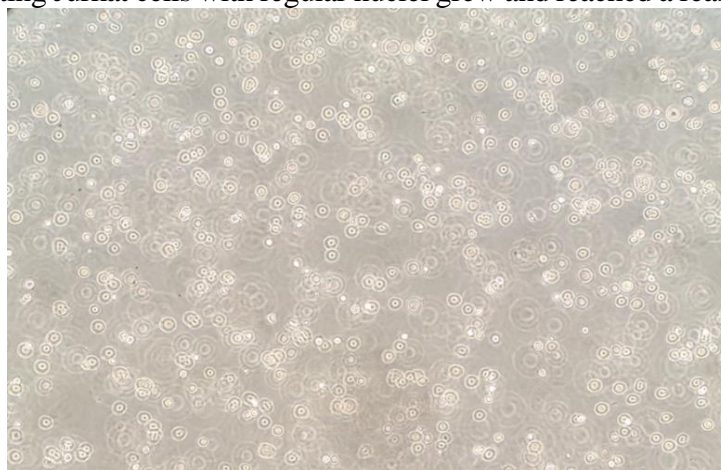


**Fig. 1.** Jurkat cell culture. Microscopic image of Jurkat cells after 48 hours show spherical cells under the inverted microscope (magnification: 40×).

### Characterization of Ag nanostructure

According to high magnification images transmission electron microscopy (TEM), the Ag-NS was rod-shaped, and the average size of the particles was 60 nm. The UV-visible spectrophotometer confirms the formation of the synthesized nano silver (rod shape). The change of nanostructure coating from CTAB to alginate was investigated by Fourier transform infrared spectroscopy (FTIR) analysis, and X-ray diffractometer (XRD) proved the presence of silver in the composition (20).

### In vitro cell viability assay

The cytotoxicity of Ag-NS was determined by MTT assay (Figs. 2A and B) at different concentrations against Jurkat cells, revealing its

potent anticancer activity against the leukemic cell line *in vitro*. Jurkat cells incubated with 25-75 µg/ml Ag-NSs decreased their viability in a dose- and time-dependent manner. According to the results of the MTT test (two-way ANOVA) in the present study at 24 hours, there were no significant difference between the control group and the experimental groups; hence, the concerned period was excluded. Moreover, the 72-hour data were less valuable than the 48-hour data because of cell doubling; hence, 48 hours was set as the optimal time point. The optimal dose for the Ag nanostructure was also 75 µg/ml since the survival of Jurkat cells was less than half the maximum inhibitory concentration (IC<sub>50</sub>) and >50%, respectively (P ≤ 0.0001, Fig. 3).

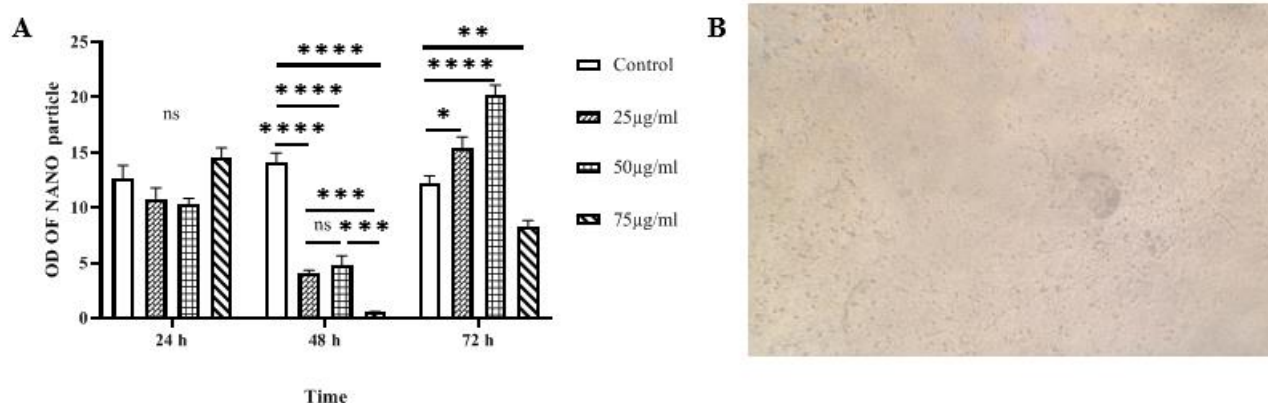


**Fig. 2.** Cytotoxicity of Ag nanostructure. **A.** Leukemic cell line was treated with different concentrations of Ag nanostructure, and MTT assay was performed after 24, 48, and 72 hours of treatment. Absorbance was measured at 570 nm and showed strong anticancer activity against these cells at a concentration of 75 µg/mL after 48 hours. All results were expressed as mean ± SD. The \* represents the values compared with the control group and the \*\*\*\* show P < 0.0001. **B.** Jurkat cells treated with an Ag nanostructure at a dose of 75 µg/ml after 48 hours (magnification: 40×).

**Gene expression results**

The expression level of the *BAX*, *BCL-2*, and *CASPASE-3* in human Jurkat cells treated with IC50 Ag-NPs compared to the control group, indicating the critical role of apoptosis following

the treatment of Jurkat cells with Ag-NS (Fig. 3). A significant increase in *BAX* (\*\*P ≤ 0.01) and *CASPASE-3* (\*P ≤ 0.05) and a significant decrease in *BCL-2* in the treated group compared to the control group (\*\*P ≤ 0.01) were found.

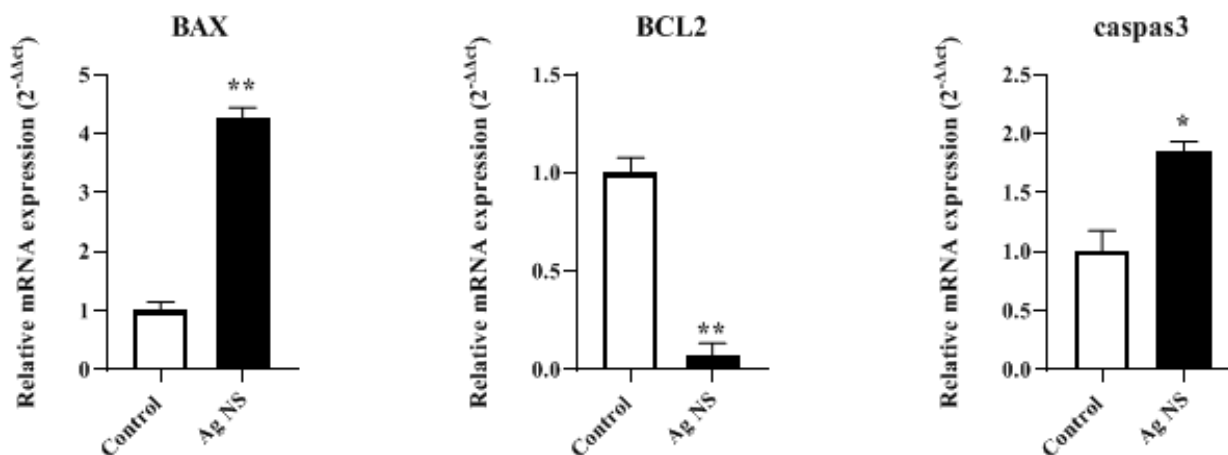


**Fig. 3.** The effects of Ag nanostructures on mRNA expression levels of apoptotic genes. The expression of *BAX* and *CASPASE-3* was upregulated in the treatment group. The expression of *BCL-2* decreased significantly in the Ag group compared with the control group. (n = 8) and GAPDH was an internal control. \*P < 0.05 and \*\*P < 0.01 compared with the control group.

**Discussion**

In this study silver nanorods was prepared and the effects of modified silver nanostructures on T-cell acute lymphoblastic leukemia were evaluated. Results from high-resolution transmission electron microscopy (HR-TEM) show that the synthesized nanostructures were rod-shaped with an average size of about 60 nm. The results of UV and XRD analyzes confirmed the synthesis of the rod-shaped

structure and the presence of silver crystals in it. The change of nanostructure coating from CTAB to alginate was also studied by FTIR analysis (20). The findings mainly revealed the induction of apoptosis in Jurkat cells by increasing the expression of proapoptotic genes and decreasing the expression of anti-apoptotic genes.

Leukemia refers to a group of aggressive and rapidly progressive cancers (22). In recent

years, NPs have been used as a clinical treatment for various diseases, including cancers. Accordingly, Ag-NPs could be a candidate for anticancer drugs (23).

In the present study, the Gold-Silver core-shell nanorods with a gold core and a silver shell were selected because of the excellent stability of Au and the aspect ratio characteristics depending on local plasmonicity. Moreover, this model of Ag-NSs has been reported to have better clinical applications. Anoop Narayanan *et al.* concluded that silver nanorods could be used as anticancer agents for colon cancer and human breast cancer cells (24). In another study, these nanorods had the increased levels of proapoptotic proteins compared to nanostars (25). In the present study, the size of the synthesized Ag NRs was about 50 nm, facilitating the diffusion of the particles into the cells due to the smaller size of the NRs. The stability of NPs is predicted using physicochemical rules. The mean of zeta potential for the Ag-NRs was about 60 mV, indicating its excellent stability. According to the literature review, the cytotoxic properties of Ag-NPs inhibit proliferation (26, 27). According to our findings, Ag-NSs induce cell death in Jurkat cells via apoptosis signaling pathway in T- ALL patients.

Apoptosis or programmed cell death is a phenomenon controlled by genes (27). In our study, the apoptotic effect of synthesized Ag-NS was investigated by analyzing the expression of the *BAX*, *BCL2*, and *CASPASE-3* genes in Jurkat cells treated with the IC50 of Ag-NS for 48 hours. One of the most common events in apoptosis is the activation of caspases. An increase in *CASPASE-3* activity demonstrated that Jurkat cells induced apoptosis following incubation with Ag-NPs (28). Moreover, Ahmadian *et al.* (29) found that treating liver hepatocellular carcinoma cell lines with nanosilver leads to the activation of *CASPASE-3* (29). According to our observations, apoptosis is induced by activating effector *caspase-3* in human Jurkat cells. *CASPASE-3* is also indispensable for some typical apoptosis hallmarks and is

required for apoptotic chromatin condensation and DNA fragmentation (30).

Regulating apoptotic biomarker genes such as *BCL-2* and *BAX* is also reported to be critical for the induction of apoptosis (31). According to our findings, the *BAX* expression is increased, indicating that the intrinsic apoptotic pathway causes cell apoptosis in Jurkat cells treated with Ag-NP. These findings are consistent with previous studies addressing other cells treated with silver nanoparticles (27, 32).

This study also showed a decrease in the *BCL-2* gene expression. The *BCL-2* family proteins are located in mitochondria and regulate apoptotic mechanisms (33). The members of this family have anti-apoptotic (including *Bcl-2*, *Bcl-xl*) and proapoptotic (including *Bax*, *Bak*) functions (34).

Variations in proapoptotic gene *BAX* and the anti-apoptotic gene *BCL-2* levels revealed that Ag-NS induced apoptosis in Jurkat cells. Due to the increased *CASPASE-3* activity, the mechanism of cell apoptosis is also dependent on an intracellular pathway.

According to the findings, Ag-NSs have anticancer properties and can induce cell apoptosis; hence, they could be a potential candidate for treating T-cell acute lymphoblastic leukemia.

## Acknowledgment

All experiments were performed in the laboratories of the Anatomy Department and Cellular and Molecular Research Center (CMRC), IUMS, Tehran, Iran. The present study was supported by Iran University of Medical Sciences (NO. 98-1-4-14209). There is no conflict of interest in this study.

## Conflicts of interest

The authors declare that they have no conflicts of interest.

## Funding

The present study was supported by Iran University of Medical Sciences (IUMS) (NO. 98-1-4-14209).

## References

1. Iacobucci I, Mullighan CG. Genetic Basis of Acute Lymphoblastic Leukemia. *J Clin Oncol*. 2017;35(9):975-983.
2. Johansson B, Harrison CJ. Acute myeloid leukemia. In: Heim S, Mitelman F, editors. *Cancer Cytogenetics*. 4th ed. Hoboken: Wiley-Blackwell; 2015;62–125
3. Hefazi M, Litzow MR. Recent Advances in the Biology and Treatment of T Cell Acute Lymphoblastic Leukemia. *Curr Hematol Malig Rep*. 2018;13(4):265-274.
4. Bene MC, Castoldi G, Knapp W, Ludwig WD, Matutes E, Orfao A, van't Veer MB. Proposals for the immunological classification of acute leukemias. European Group for the Immunological Characterization of Leukemias (EGIL). *Leukemia*. 1995;9(10):1783-6.
5. Pui CH, Thiel E. Central nervous system disease in hematologic malignancies: historical perspective and practical applications. *Semin Oncol*. 2009;36(4 Suppl 2):S2-S16.
6. Ghodousi-Dehnavi E, Arjmand M, Akbari Z, Aminzadeh M, Haji Hosseini R. Anti-Cancer Effect of *Dorema Ammoniacum Gum* by Targeting Metabolic Reprogramming by Regulating *APC*, *P53*, *KRAS* Gene Expression in HT-29 Human Colon Cancer Cells. *Rep Biochem Mol Biol*. 2023;12(1):127-135.
7. Rezai M, Saravani R, Sargazi S, Moudi M, Jafari Shahroudi M, Saravani R. *Achillea Wilhelmsii C. Koch* Hydroalcoholic Extract Induces Apoptosis and Alters *LIN28B* and *p53* Gene Expression in Hela Cervical Cancer Cells. *Rep Biochem Mol Biol*. 2019;8(3):318-325.
8. Elmore S. Apoptosis: a review of programmed cell death. *Toxicol Pathol*. 2007;35(4):495-516.
9. Nikolettou V, Markaki M, Palikaras K, Tavernarakis N. Crosstalk between apoptosis, necrosis and autophagy. *Biochim Biophys Acta*. 2013;1833(12):3448-3459.
10. Gholipour H, Lahijani MS. Teratogenic Effects of Two New Derivatives of Quinazolinones on Balb/C Mice Embryos and Newborns: A Literature Review. *Curr Res Biol*. 2017;9(2):23-31.
11. Chipuk JE, Moldoveanu T, Llambi F, Parsons MJ, Green DR. The BCL-2 family reunion. *Mol Cell*. 2010;37(3):299-310.
12. Sánchez-López E, Gomes D, Esteruelas G, Bonilla L, Lopez-Machado AL, Galindo R, et al. Metal-Based Nanoparticles as Antimicrobial Agents: An Overview. *Nanomaterials (Basel)*. 2020;10(2):292.
13. Sofi MA, Sunitha S, Sofi MA, Pasha SKK, Choi D. An overview of antimicrobial and anticancer potential of silver nanoparticles. *J King Saud Univ Sci*. 2022;34 (2).101791.
14. Cheng X, Zhang W, Ji Y, Meng J, Guo H, Liu J, et al. Revealing silver cytotoxicity using Au nanorods/Ag shell nanostructures: disrupting cell membrane and causing apoptosis through oxidative damage. *RSC Adv*. 2013;3(7):2296-305.
15. Mikhailova EO. Silver Nanoparticles: Mechanism of Action and Probable Bio-Application. *J Funct Biomater*. 2020;11(4):84.
16. Franco-Molina MA, Mendoza-Gamboa E, Sierra-Rivera CA, Gómez-Flores RA, Zapata-Benavides P, Castillo-Tello P, et al. Antitumor activity of colloidal silver on MCF-7 human breast cancer cells. *J Exper Clin Cancer Res*. 2010;29(1):148.
17. Asharani P, Hande MP, Valiyaveetil S. Anti-proliferative activity of silver nanoparticles. *BMC Cell Biol*. 2009;10(65):1-14.
18. Guo D, Zhao Y, Zhang Y, Wang Q, Huang Z, Ding Q, et al. The cellular uptake and cytotoxic effect of silver nanoparticles on chronic myeloid leukemia cells. *J Biomed Nanotechnol*. 2014;10(4):669-78.
19. Lee YH, Cheng FY, Chiu HW, Tsai JC, Fang CY, Chen CW, Wang YJ. Cytotoxicity, oxidative stress, apoptosis and the autophagic

effects of silver nanoparticles in mouse embryonic fibroblasts. *Biomaterials*. 2014;35(16):4706-15.

20. Nazari M, Shabani R, Ajdary M, Ashjari M, Shirazi R, Govahi A, Kermanian F, Mehdizadeh M. Effects of Au@Ag core-shell nanostructure with alginate coating on male reproductive system in mice. *Toxicol Rep*. 2023;10:104-116.
21. Govahi A, Amjadi F, Nasr-Esfahani MH, Raoufi E, Mehdizadeh M. Accompaniment of Time-Lapse Parameters and Cumulus Cell RNA-Sequencing in Embryo Evaluation. *Reprod Sci*. 2022;29(2):395-409.
22. Chiaretti S, Gianfelici V, O'Brien SM, Mullighan CG. Advances in the Genetics and Therapy of Acute Lymphoblastic Leukemia. *Am Soc Clin Oncol Educ Book*. 2016;35:e314-22.
23. Zhang XF, Liu ZG, Shen W, Gurunathan S. Silver Nanoparticles: Synthesis, Characterization, Properties, Applications, and Therapeutic Approaches. *Int J Mol Sci*. 2016;17(9):1534.
24. Anoop NV, Jacob R, Paulson JM, Dineshkumar B, Narayana CR. Mango leaf extract synthesized silver nanorods exert anticancer activity on breast cancer and colorectal carcinoma cells. *J Drug Deliv Sci Technol*. 2018;44:8-12.
25. Steckiewicz KP, Barcinska E, Malankowska A, Zauszkiewicz-Pawlak A, Nowaczyk G, Zaleska-Medynska A, Inkielewicz-Stepniak I. Impact of gold nanoparticles shape on their cytotoxicity against human osteoblast and osteosarcoma in in vitro model. Evaluation of the safety of use and anti-cancer potential. *J Mater Sci Mater Med*. 2019;30(2):22.
26. Zhou G, Wang W. Synthesis of silver nanoparticles and their antiproliferation against human lung cancer cells in vitro. *Orient J Chem* 2012;28(2):651-55.
27. Baharara J, Namvar F, Ramezani T, Mousavi M, Mohamad R. Silver nanoparticles biosynthesized using *Achillea biebersteinii* flower extract: apoptosis induction in MCF-7 cells via caspase activation and regulation of Bax and Bcl-2 gene expression. *Molecules*. 2015;20(2):2693-706.
28. Mollick MMR, Rana D, Dash SK, Chattopadhyay S, Bhowmick B, Maity D, et al. Studies on green synthesized silver nanoparticles using *Abelmoschus esculentus* (L.) pulp extract having anticancer (in vitro) and antimicrobial applications. *Arab J Chem*. 2019;12(8):2572-84.
29. Ahmadian E, Dizaj SM, Rahimpour E, Hasanzadeh A, Eftekhari A, Hosain Zadehan H, et al. Effect of silver nanoparticles in the induction of apoptosis on human hepatocellular carcinoma (HepG2) cell line. *Mater Sci Eng C Mater Biol Appl*. 2018;93:465-471.
30. Porter AG, Jänicke RU. Emerging roles of caspase-3 in apoptosis. *Cell Death Differ*. 1999 Feb;6(2):99-104.
31. Singh R, Letai A, Sarosiek K. Regulation of apoptosis in health and disease: the balancing act of BCL-2 family proteins. *Nat Rev Mol Cell Biol*. 2019;20(3):175-193.
32. Ghooshchian M, Khodarahmi P, Tafvizi F. Apoptosis-mediated neurotoxicity and altered gene expression induced by silver nanoparticles. *Toxicology and Industrial Health*. 2017;33(10):757-764.
33. Gross A. BCL-2 proteins: regulators of the mitochondrial apoptotic program. *IUBMB Life*. 2001;52(3-5):231-6.
34. Renault TT, Dejean LM, Manon S. A brewing understanding of the regulation of Bax function by Bcl-xL and Bcl-2. *Mech Ageing Dev*. 2017;161(Pt B):201-210.